A STUDY OF DEPTH INACCURACY IN TIME-OF-FLIGHT (TOF) CAMERAS CAUSED BY COLOR VARIATIONS OF OBJECTS

Alexandar Lyubenov [1], Stefan Ivanov[2]

[1] *TU-Gabrovo*
[2]*TU-Gabrovo*

Abstract

Time-of-Flight (ToF) cameras represent 3D imaging sensors capable of providing both depth and amplitude images at a high frame rate. The rapid evolution of this technology in recent years has been noteworthy. However, the effectiveness of ToF cameras is contingent upon imaging conditions and external factors, rendering the captured data susceptible to inaccuracies. This study delves into the impact of color and distance on the depth accuracy of ToF cameras. Our experiments unveiled the diverse effects of color and distance on the depth inaccuracies inherent in ToF cameras. Nevertheless, due to the varied nature of these faults, a unified description is unattainable. Addressing these inaccuracies necessitates a robust foundation of experimental data, which is the primary objective of this research. The findings will serve as a crucial resource for future algorithms aimed at rectifying these anomalies.

Keywords: ToF camera, depth error, error modeling, error correction.

INTRODUCTION

Time-of-Flight (ToF) cameras, a rapidly evolving category of 3D imaging sensors, offer a depth and amplitude image with a high frame rate. Their compact structure, light weight, and low power consumption make them ideal for diverse applications, including ground robot navigation [1], pose estimation [2], 3D object reconstruction [3], and human organ identification and tracking [4]. Despite these advantages, ToF cameras are susceptible to inaccuracies in their collected data due to imaging limitations and external interference.

One notable inaccuracy arises from the absence of a consistent technique to correct non-systematic inaccuracies introduced by the external environment [5]. Consequently, various depth errors must be individually examined, modeled, and rectified based on their diverse causes.

ToF camera errors are broadly categorized into systematic and non-systematic errors. Systematic errors exhibit a relatively constant shape, often resulting from imaging circumstances, and can be evaluated and rectified with relative simplicity. On the other hand, non-systematic errors are random and influenced by noise and the surrounding environment, making it challenging to develop a single model for explanation and correction. The four main types of non-systematic errors include signal-to-noise ratio, multiple light reception, light scattering, and motion blurring [5].

To mitigate signal-to-noise ratio errors, low amplitude filtering or advanced algorithms for optimal integration time determination are viable options [6,7]. Various approaches, such as computing data averages and setting limits, can reduce the impact of noise [8, 9, 10]. Multiple light reception errors are most common at the surface edges and depressions of the target object. While incidence angle comparison can eliminate errors at surface edges [7, 11, 12], addressing inaccuracies in depressions remains a challenge.

Other papers focus on the non-systematic errors of ToF cameras, commencing with an analysis of the influence of external distractions like materials, colors, distances, and lighting on depth errors [5]. The subsequent sections provide an overview of the principle and development of ToF cameras and a detailed analysis of the impact of lighting, material properties, color, and distance on depth errors through sets of experiments [5].

DEVELOPMENT AND PRINCIPLE OF TOF CAMERAS

The inception of ToF cameras dates back to 1977 at the Stanford Research Institute (SRI) . However, this approach wasn't widely adopted initially due to limitations imposed by detector technology of that era. It wasn't until the 1990s that rapid light sampling became feasible with the development of lock-in CCD (Charge-Coupled Device) technology. In 1997, Schwarte, a researcher at the University of Siegen (Germany), introduced a method based on lock-in CCD technology for determining the phases and/or magnitudes of electromagnetic waves. His team successfully developed the first ToF camera prototype using this method, marking a significant milestone in the advancement of ToF cameras.

Subsequently, with the advent of lock-in CCD technology and innovative methodologies, ToF cameras experienced rapid development, paving the way for their widespread application in various fields.

The operation of ToF cameras is illustrated in Figure 1. Initially, a modulated signal is emitted onto the surface of the target object, typically using a light source such as an LED. Subsequently, the sensor measures the accumulated charge numbers for each pixel. Through this measurement, the phase shift between the transmitted and received signals is determined. This process enables the calculation of the distance between the ToF camera and the target object, providing information about the object's proximity.

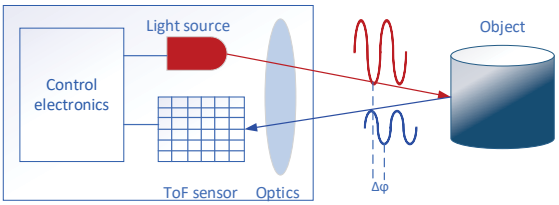

Fig. 1. *ToF sensor principle of operation*

A ToF sensor employs a method to estimate the distance between the sensor and an object. In this approach, the sensor emits a signal that reflects off the object, allowing it to discern when a complete round trip has occurred. Typically, the signal can be generated using either light or sound waves. In both cases, the following equation is utilized to calculate the distance or range:

$$R = v*\Delta T/2 \qquad (1)$$

where:

- R represents the range (in meters),
- v is the wave propagation velocity (in meters per second), and
- ΔT is the round-trip time (in seconds).

Dividing by 2 simplifies the round-trip time to the time it takes for the signal to travel from the sensor to the object.

In the context of air, the speed of light, which is approximately 3.10^8 meters per second, enables a broader range and quicker measurements compared to sound.

ToF cameras find utility in various applications beyond well-known ToF sensing uses in smartphones and moving automobiles, such as parking and accident-avoidance systems. They are also valuable for people counting applications. Moreover, in confined spaces like silos, vats, or tanks, Time-of-Flight level sensing technology presents a completely non-contact alternative to traditional mechanical and capacitive level detection methods. This technology proves particularly advantageous in scenarios where a contactless approach is preferred or where the conditions might be challenging for mechanical or capacitive systems.

ANALYSIS ON DEPTH ERRORS OF TOF CAMERAS

Developing a comprehensive model to elucidate and rectify errors in Time-of-Flight (ToF) cameras can be challenging due to the typically random and unclear influence of the external environment on these cameras. In this section, we delve into an analysis of how transformations in the external environment affect the depth error of ToF cameras, employing the PMD flexx1 3D Camera. The insights derived from these tests are instrumental in guiding the correction of depth inaccuracies in future endeavors. This examination serves as a crucial reference point for refining ToF camera performance under varying external conditions.

The outcomes of this study aim to provide valuable insights into the influence of surface color on the accuracy of depth measurements.

A planned experimental setup was employed to assess the Time-of-Flight (ToF) sensor's ability to differentiate between various hues. A paper sheet utilized in the study was printed with a distinct color sample, and it was arranged on a transparent plexiglass surface. During the experiment, the sensor emitted a modulated IR light signal toward the color sample, measuring the time it took for the light to return to the sensor. Subsequent processing of the data gathered from these measurements yielded precise distance information.

The ColorChecker Color Rendition Chart, commonly known as the Macbeth ColorChecker or simply the Macbeth chart, is a standardized instrument extensively employed in photography, cinematography, and color science for evaluating and calibrating the color accuracy of imaging systems. Originally developed by Kollmorgen Instruments Corporation's Macbeth Division, it has evolved to become a widely recognized and utilized reference in the realms of color management and color reproduction.

Comprising a grid of 24 color patches, each with a distinct and precisely defined color, the Macbeth chart (Fig.2) spans a broad spectrum of colors and saturation levels. This spectrum includes primary and secondary colors, along with various shades of gray. The construction of the chart often employs premium materials to ensure the stability of its colors over time.

***Fig. 2** Machbeth ColorChecker*

Throughout this research study, a examination of a Time-of-Flight (ToF) sensor's ability to differentiate between various colors on a single sheet of paper was conducted. The experimental setup featured twenty-four distinct color types, including black and white. The printed sheet presented a complex checkerboard pattern, each color block containing a combination of numbers, letters, and special symbols. This intricate design aimed to evaluate the sensor's capacity to differentiate not only between colors but also intricate details within color blocks, enriching the assessment of its color recognition capabilities.

EXPERIMENT

In the context of this research study, an assessment was conducted to evaluate the color differentiation capabilities of a Time-of-Flight (ToF) sensor when tasked with recognizing distinct colors printed on a sheet of paper at short distance in front of the sensor. The experiment sought to investigate the sensor's ability to discern colors across varying distances. Initially, the ColorChecker pattern was positioned at a distance of 10 centimeters from the ToF sensor, well within its typical range. As expected, the sensor effectively recognized and differentiated some colors under these conditions. However, as the pattern was progressively moved farther away, extending up to a distance of 1 meter, a

notable limitation became apparent. The ToF sensor exhibited a diminishing capacity to recognize colors beyond the range of 30-60 centimeters. These experiments collectively provided valuable insights into the sensor's range limitations and its capacity for color recognition at various distances and angles, crucial considerations for applications demanding precise color detection and object recognition in diverse scenarios.

The developed template using the Macbeth ColorChecker as a reference is presented in Fig.3.

Fig.3 *Test template*

When the test pattern is positioned in front of the ToF sensor, and its position is measured and read by the sensor, an interesting observation is made. At close distances, some colors in the test pattern do not reflect the infrared light directed towards them. Consequently, for these specific colors, the data measured by the sensor lacks information about their distance, as depicted in Figure 4. This phenomenon highlights a limitation in the sensor's ability to capture distance information for certain colors, particularly at close proximity. Understanding such nuances is crucial for refining and optimizing the ToF sensor's performance in scenarios where accurate distance measurement for diverse colors is essential.

Fig.4 *Test pattern in close proximity to the ToF sensor*

In addition to the observed loss of detection for certain colors, another notable finding indicates a slight discrepancy in the measured distance to the color pattern for the different colors that the sensor successfully detects. This discrepancy suggests variations in the sensor's ability to accurately measure distances based on different colors. Such insights into color-specific distance measurement discrepancies are essential for understanding the sensor's performance nuances and can inform further refinements in its calibration and functionality.

As the test pattern moves away from the sensor, the individual impact of colors on the sensor's performance diminishes. At greater distances, the sensor consistently determines the distance to the color template without losing data for different colors. Figure 5 illustrates the operation of the ToF sensor when the template is positioned more than a meter from it. This observation indicates that, at increased distances, the sensor's ability to uniformly measure distance becomes more prominent, reducing the influence of individual colors on its performance. Understanding these dynamics is crucial for interpreting the ToF sensor's behavior at varying distances and optimizing its performance for diverse scenarios.

Fig.5 *The test pattern away from the sensor*

The distances at which the ToF sensor starts receiving information from the respective colors and determines the distance to them are measured and summarized in Table 1.

This table provides valuable insights into the sensor's color-specific detection range and its ability to capture distance information for different colors at varying distances from the sensor.

Table.1

Color name	Color code	Detection distance, cm
Dark skin A	#735244	under 10
Light skin Б	#c29682	50
Blue sky Ш	#627a9d	50
Foliage Г	#576c43	20
Blue flower Д	#8580b1	40
Bluish green E	#67bdaa	40
Orange +	#d67e2c	40
Purplish blue §	#505ba6	20
Moderate red %	#c15a63	50
Purple @	#5e3c6c	under 10
Yellow green $	#9dbc40	40
Orange yellow	#e0a32e	40
Blue A	#383d96	under 10
Green b	#469449	40
Red C	#af363c	30
Yellow d	#e7c71f	40
Magenta E	#bb5695	30
Cyan F	#0885a1	30
White 1	#f3f3f2	40
Neutral 8 2	#c8c8c8	40
Neutral 6.5 3	#a0a0a0	40
Neutral 5 4	#7a7a7a	30
Neutral 3.5 5	#555555	under 10
Black 6	#343434	under 10

The table reveals that certain colors, particularly at close distances, pose challenges for the accurate determination of the distance to the objects. On the other hand, for other colors, this issue is either absent or not expressed to the same extent. This disparity underscores the color-specific performance variations of the ToF sensor, emphasizing the importance of understanding how different colors influence its distance measurement accuracy, especially in close proximity scenarios.

Considering that the measurements were conducted using a color test pattern printed on regular printer paper, future research will explore how colors in various materials impact the accuracy of objects in close proximity to the ToF sensor. Understanding the material-specific influence on the sensor's performance can provide valuable insights for real-world applications where diverse materials may be encountered.

Furthermore, another avenue for future research involves investigating how the angle at which the test pattern is positioned relative to the ToF sensor affects the data obtained. Exploring the impact of different angles on the sensor's measurements can contribute to a comprehensive understanding of its behavior in varying spatial orientations. This knowledge is essential for optimizing the sensor's performance in practical scenarios where objects may not always be aligned perpendicular to the sensor.

CONCLUSION

The present study focused on examining the impact of different colors on the performance of a Time-of-Flight (ToF) sensor in determining objects located at close distances. The results obtained in this research offer valuable insights that can be leveraged in the development of algorithms aimed at evaluating the reliability of sensor readings when objects are in close proximity. Additionally, these findings can contribute to the exploration of methods and approaches to

compensate for noises and information gaps in the data received from the sensor.

While additional extensive studies are warranted to fully understand the nuances of the ToF sensor's performance for close objects, the insights provided in this work reveal interesting features in the sensor's behavior. These identified characteristics can serve as a foundation for developing algorithms designed to mitigate and compensate for specific challenges encountered in close-distance scenarios. This study lays the groundwork for future research and advancements in improving the accuracy and robustness of ToF sensors in proximity detection applications.

REFERENCE

[1] Schars tein, D.; Szeliski, R. A taxonomy and evaluation of dense two-frame stereo correspondence algorithms. Int. J. Comput. Vision, 2002, 47, 7-42.

[2] Hansard, M.; Lee, S.; Choi, O.; and Horaud, R.P. Time-of-flight cameras: principles, methods and applications. Springer: Cham, Switzerland, 2012.

[3] Kim, S.; Cho, J.; Koschan, A.; Abidi, M. Spatial and temporal enhancement of depth images captured by a time-of-flight depth sensor. In Proceedings of the 20th International Conference on Pattern Recognition, Istanbul, Turkey, 23–26 August 2010.

[4] Foix, S.; Alenya, G.; Torras, C. Lock-in time-of-flight (ToF) cameras: a survey. IEEE Sens. J. 2011, 11, 1917- 1926.

[5] Mure-Dubois, J.; Hügli, H. Real-time scattering compensation for time-of-flight camera. Available online: http://biecoll.ub.uni-bielefeld.de/index.php/icvs/article/view/240 (11 September 2019).

[6] Fuchs S. Multipath interference compensation in time-of-flight camera images. In Proceedings of the 20th International Conference on Pattern Recognition, Istanbul, Turkey, 23–26 August 2010

[7] Reynolds, M.; Doboš, J.; Peel, L.; Weyrich, T.; Brostow, G. J. Capturing time-of-flight data with confidence. In Proceedings of the IEEE Computer Vision and Pattern Recognition, Providence, RI, USA, 20–25 June 2011

[8] Agresti, G.; Minto, L.; Marin, G.; Zanuttigh, P. Stereo and ToF data fusion by learning from synthetic data. Inf. Fusion 2019, 49, 161–173.

[9] Wang, A.; Qiu, T.; Shao, L. A simple method of radial distortion correction with centre of distortion estimation. J. Math. Imaging Vision, 2009, 35, 165172

[10] Song, Y.; Ho, Y. High-resolution depth map generator for 3D video applications using time-of-fligh

[11] Kim, S.; Cha, J.; Ryu, J.; Lee, K. Depth video enhancement of haptic interaction using a smooth surface reconstruction. IEICE Trans. Inf. Syst. 2006, 89, 37–44.

[12] Zhu, J.; Wang, L.; Yang, R.; Davis, J. Fusion of time-of-flight depth and stereo for high accuracy depth maps. In Proceedings of the 2008 IEEE Conference on Computer Vision and Pattern Recognition, Anchorage, AK, USA, 23–28 June 20082.

[13] LEE, J.; PARK, H. Efficient synthesis-based depth map coding in AVC-compatible 3D video coding. IEEE Trans. Circuits Syst. Video Technol. 2015, 26, 1107–1116.

[14] Ho, Y.; Lee, E.; Lee, C. Multiview video test sequence and camera parameters. Available online: https://www.researchgate.net/publication/259756600_Contribution_Poznan_Multiview_Video_Test_Sequences_and_Camera_Parameters(1 February 2019).

[15] Tomasi, C.; Manduchi, R. Bilateral filtering for gray and color images. In Proceedings of the Sixth International Conference on Computer Vision, Bombay, India, 7–7 January 1998.

[16] Kopf, J.; Cohen, M. F.; Lischinski, D.; Uyttendaele, M. Joint bilateral upsampling. ACM Trans. Graphics 2007, 26, doi:10.1145/1276377.1276497

[17] Matyunin, S.; Vatolin, D.; Berdnikov, Y.; Smirnov, M. Temporal Filtering for Depth Maps generated by Kinect Depth Camera. In Proceedings of the 3DTV Conference: The True Vision - Capture, Transmission and Display of 3D Video (3DTV-CON), Antalya, Turkey, 16–18 May 2011

[18] Garcia, F.; Aouada, D.; Mirbach, B.; Ottersten, B. Spatio-temporal ToF data enhancement by fusion In Proceedings of

the 19th IEEE International Conference on Image Processing, Orlando, FL, USA, 30 September–3 October 2012
[19] Zhang Z. A flexible new technique for camera calibration. IEEE Trans. Pattern Anal. Mach. Intell., 2000, 22, 1330–1334.
[20] Huang, T.; Yang, G.; Tang, G. A fast two-dimensional median filtering algorithm. IEEE Trans. Acoust. Speech Signal Process. 1979, 27, 13–18.
[21] Yin, L.; Yang, R.; Gabbouj, M.; Neuvo, Y. Weighted median filters: a tutorial. IEEE Trans. Circuits Syst. II: Analog Digital Signal Process 1996, 43, 157–192
[22] Ma, Z.; He, K.; Wei, Y.; Sun, J.; Wu, E. Constant time weighted median filtering for stereo matching and beyond. Available online: https://www.cv-foundation.org/openaccess/content_iccv_2013/html/Ma_Constant_Time_Weighted_2013_ICCV_paper.html, (1 February 2019).
[23] Middlebury stereo vision page, Available online: http://vision.middlebury.edu/stereo/, Dec. 2001..
[24] Xu, L.; Yan, Q.; Xia, Y.; Jia, J. Structure extraction from texture via relative total variation. ACM Trans. Graphics 2012, 31, doi.org/10.1145/2366145.2366158
[25] Gastal, E. S.; Oliveira, M. M. Domain Transform for Edge-Aware Image and Video Processing. ACM Trans. Graphics 2011, 30, 69:1–69:12.